

Microseismic event classification with a lightweight Fourier Neural Operator model

Ayrat Abdullin¹, Umair bin Waheed^{1,*}, Leo Eisner², and Abdullatif Al-Shuhail¹

¹King Fahd University of Petroleum and Minerals, Department of Geosciences, Dhahran, 31261, Saudi Arabia

²Seismik s.r.o., Prague, 18200, Czech Republic

*umair.waheed@kfupm.edu.sa

ABSTRACT

Real-time monitoring of induced seismicity is crucial for mitigating operational hazards, relying on the rapid and accurate classification of microseismic events from continuous data streams. However, while many deep learning models excel at this task, their high computational requirements often limit their practical application in real-time monitoring systems. To address this limitation, a lightweight model based on the Fourier Neural Operator (FNO) is proposed for microseismic event classification, leveraging its inherent resolution-invariance and computational efficiency for waveform processing. In the STanford EArthquake Dataset (STEAD), a global and large-scale database of seismic waveforms, the FNO-based model demonstrates high effectiveness for trigger classification, with an F1 score of 95% even in the scenario of data sparsity in training. The new FNO model greatly decreases the computer power needed relative to current deep learning models without sacrificing the classification success rate measured by the F1 score. A test on a real microseismic dataset shows a classification success rate with an F1 score of 98%, outperforming many traditional deep-learning techniques. A combination of high success rate and low computational power indicates that the FNO model can serve as a methodology of choice for real-time monitoring of microseismicity for induced seismicity. The method saves computational resources and facilitates both post-processing and real-time seismic processing suitable for the implementation of traffic light systems to prevent undesired induced seismicity.

Introduction

It is well-documented that the injection or extraction of fluids in subsurface geological formations can trigger induced seismicity¹. Fluid injection typically induces geomechanical instability by reducing the effective normal stress due to increased pore pressure². In addition, induced seismicity may also result from other mechanisms, such as fault reactivation triggered by cooling³, reservoir compaction^{4,5}, or stress redistribution⁶. The diverse mechanisms capable of initiating seismic events, combined with uncertainties regarding subsurface conditions, including stress fields, thermal gradients, and fault geometry, result in limited *a priori* predictability of induced seismicity regarding its spatial occurrence, timing, and magnitude.

Such hazards are reduced by seismic monitoring with real-time detection and characterization of induced seismicity during anthropogenic operations⁷. The seismic event characterization requires triggering, classification of triggers, and phase picking, which is a challenge in both earthquake seismology and microseismic monitoring. Traditionally, seismic analysts have determined earthquake signals by visually inspecting three components of waveforms of multiple stations and manually selecting P- and S-wave phase arrivals. However, this method is time-consuming and prone to errors. In particular, these tasks are difficult for microseismic monitoring due to the typically low magnitudes of microseismic events and their susceptibility to noise interference. Visual detection is impractical in real-time operations, and the growing volume of seismic data makes manual analysis impossible, requiring automated algorithms. The most commonly used algorithms for event detection (i.e., triggering and classification) are STA/LTA⁸ and template matching⁹. Although STA/LTA provides computational efficiency, its sensitivity to low-magnitude events and time-varying noise is limited, and its performance is somewhat subjective as it depends on the choice of STA/LTA parameters. The subjectivity of STA/LTA detection is overcome by selecting low thresholds in STA/LTA detection, resulting in a high rate of triggers with false detections. Hence, the triggers need to be classified into true and false detections. Template matching, on the other hand, is robust in detecting small events, but struggles with waveform variability and high computational requirements, making it difficult to apply in real-time¹⁰. Furthermore, the template matching requires previously recorded events - the templates - rarely available at induced seismicity monitoring.

With the growing interest in the potential of machine learning (ML) in the seismological community, significant efforts have been devoted to improving the capabilities of event identification. The application of ML to seismic event classification and detection has been studied since the 1990s, and many methodologies have been proposed. Many of these approaches use artificial neural networks applied to features extracted from recorded seismic signals¹¹⁻¹³. We note that these algorithms

are applied to stationary networks with previously recorded seismicity, which is used for training. With the development and widespread availability of computational resources, deep learning (DL) has become a transformative tool for solving long-standing problems in science and engineering disciplines, including event detection and classification in seismology. In recent years, several deep learning models for detection and phase picking have been published^{14–18}. Existing deep learning models applied to seismic data analysis differ in several key dimensions, including network architecture, such as convolutional, recurrent, and attention-based frameworks; data input representation, either in the time or frequency domain; and output labeling methods, ranging from discrete point predictions to continuous sequence labeling. In addition, these models vary substantially in complexity and depth, ranging from relatively shallow configurations to significantly deeper architectures.

Various supervised DL methods have been developed, which can be classified based on the type of information they provide, from determining whether an event occurs in a triggered interval of data (classification) to determining the arrival time of the event (picking). Several binary window classification approaches have been developed, in which DL models analyze a time window to predict the presence or absence of an event. For example, Wilkins et al. (2020) developed a custom convolutional neural network (CNN) to detect microseismic events associated with mining operations, achieving a ten-fold increase in event detection compared to human experts¹⁹. Although earlier methods often focused on individual geophones, Shaheen et al. (2021) presented a CNN-based approach to detect small-magnitude events using data from an entire shallow borehole network in Groningen, the Netherlands²⁰. In addition, Ross et al. (2018) proposed a generalized phase detection (GPD) method by training a CNN on manually labeled data from the Southern California seismic network to classify data intervals as containing P-waves, S-waves, or noise¹⁴.

Both non-neural and neural network (NN) approaches have shown significant advantages over traditional trace-based detection methods. Chen (2020) presented an unsupervised fuzzy clustering method that utilizes features such as STA/LTA triggers, interval powers and means to achieve robust microseismic event detection even in high-noise environments²¹. Meanwhile, Zheng et al. (2018) and Birnie and Hansteen (2022) used recurrent long short-term memory (LSTM) neural network architectures^{22,23}. Zheng et al. (2018) trained their LSTM model on laboratory-simulated microseismic events and successfully applied it to field data²². Birnie and Hansteen (2022) further improved the LSTM model by incorporating bidirectionality and training it on various synthetic datasets with band-pass noise²³. Mousavi et al. (2019) developed a CNN-RNN earthquake detector (CRED) that combines convolutional layers with bidirectional LSTM blocks in the residual structure to improve microearthquake detection¹⁵. Using a different approach, Birnie et al. (2021) treated detection as a semantic segmentation problem for the array records, where seismic data are represented as images, and the network predicts the presence of an event at each pixel²⁴. More recently, Awais et al. (2023) demonstrated that combining super-virtual refraction interferometry with the unsupervised DBSCAN clustering algorithm enables accurate and automatic first-break traveltimes picking even in noisy seismic data sets²⁵.

Neural operators, as extensions of neural networks, are very effective in constructing surrogate models for various scenarios governed by partial differential equations (PDEs)²⁶. The Fourier neural operator (FNO)²⁷, in particular, excels at training and generalizing PDEs from data. Unlike conventional numerical solvers that solve a single instance of the PDE, the proposed FNO-based approach provides a resolution-invariant solution to the event detection and classification problem, improving both accuracy and efficiency.

Most deep learning models require a high number of trainable parameters on the order of hundreds of thousands. This, in turn, leads to increasing computational resources and time needed to train such a model. Deploying models with millions of parameters significantly reduces their practicality, particularly in applications demanding real-time data processing, such as microseismic event detection and phase picking. One of our goals in this study is to explore lightweight neural operator models with less computational burden. In the end, reducing the complexity of the computational models leads to less environmental impact, including carbon emissions and pollution.

In this study, we propose a lightweight seismic signal detection model based on FNO. We first apply the FNO framework to classify seismic events from the STanford EArthquake Dataset (STEAD)²⁸. We train and evaluate FNO on real earthquake datasets, demonstrating high accuracy. Then we train and test our algorithm on real microseismic data with further improved performance. We also benchmark this method with leading DL algorithms widely used in the seismological community^{17,29}. Showing similar performance with PhaseNet, our model has much fewer trainable parameters, which on a large scale, leads to less computation burden both in training and testing large amounts of seismic data. These results highlight the benefits of using FNO for seismic event detection, paving the way for near real-time and cost-effective microseismic monitoring capabilities.

Data and Methods

Datasets

For this study, we first used data from the STanford EArthquake Dataset (STEAD)²⁸ to analyze seismic events. The dataset is a comprehensive, globally acquired collection of seismic signals covering both local earthquakes and non-earthquake events

(seismic noise) classified by humans. It includes approximately 1.2 million three-component seismograms, totaling more than 19,000 hours of seismic recordings. The data were acquired by a network of 2,613 seismic instruments around the world, located within a 350 km radius of recorded earthquakes. Each sample consists of 6,000 data points recorded over one minute at a sampling rate of 100 Hz, and three channels: east-west (E), north-south (N), and vertical (Z). The dataset is carefully labeled, facilitating the development and evaluation of machine learning models for earthquake detection and classification. STEAD serves as a valuable resource for improving automated seismic event analysis and real-time monitoring capabilities for large earthquakes.

This study also utilizes microseismic datasets, which comprise triggered microseismic waveforms recorded during hydraulic fracturing operations. The monitoring array consisted of nine three-component surface seismic sensors distributed across an approximate 100 km² surface area, operating at a sampling frequency of 250 Hz. We downsample the dataset to a 100 Hz sampling rate, as this is the original sampling rate used for all models evaluated here, and the majority of the observed seismic signal is below 50 Hz. Although the triggered dataset contains no false seismic events, some waveform records from individual stations are noisy and lack manual phase picks. The final processed dataset consists of approximately 5,400 waveform segments from approximately 600 manually labeled seismic events, encompassing both local and near seismic events. The near seismic events are typically located at distances greater than 10 km from the nearest recording station.

Pre-trained Models

We evaluate five models for the microseismic event classification task using their original model weights (Table 1). All models are originally trained and tested here on single-station three-component data. The model architectures and weights are available in the SeisBench³⁰.

Table 1. Comparison of the deep learning models

| | FNO | CRED | DPP | EQT | GPD | PhaseNet |
|-----------------------------|--------------|------------------------------|-----------------------|------------------------|---------------------|----------------------|
| # Params | 34,000 | 293,569 | 199,731 | 376,935 | 1,741,003 | 268,443 |
| Type | NO | CNN-RNN | CNN | CNN-RNN-Attention | CNN | U-Net |
| Training set | Microseismic | N. California | INSTANCE | STEAD | S. California | N. California |
| Station spacing (km) | 5-10 | 10-30 | 25-30 | 10-30 | 10-20 | 10-30 |
| Earthquake depth (km) | 1.7-2.4 | 0.0-15.0 | 5.0-15.0 | 0.0-15.0 | 2.0-15.0 | 0.0-15.0 |
| Earthquake magnitude | 0.5-2.5 | 0.5-3.5 | 2.0-4.0 | 0.5-3.0 | 0.0-2.5 | 0.5-3.5 |
| Orig. train size (# events) | 200 | 440,000 | 65,700 | 1,100,000 | 3,375,000 | 623,000 |
| Orig. weights | Yes | Yes | No | Yes | Yes | Yes |
| Reference | This paper | (Mousavi, Zhu, et al., 2019) | (Soto & Schurr, 2021) | (Mousavi et al., 2020) | (Ross et al., 2018) | (Zhu & Beroza, 2019) |

Note: "# of parameters" refers to the total number of trainable parameters; minor deviations from the original data are possible due to differences in implementation methods. "Training size" indicates the approximate number of examples used to train the original model. "Original weights" indicates whether the weights of the original pre-trained model are available in SeisBench.

The CNN-RNN Earthquake Detector (CRED) is designed exclusively for earthquake detection (i.e., trigger and classification) and does not support seismic phase identification or phase picking¹⁵. Inputs into the network are spectrograms of three-component seismograms. CRED analyzes spectrogram representations of seismic waveforms with durations of 30 seconds, sampled at 100 Hz. Its internal architecture integrates convolutional neural network (CNN) layers followed by long short-term memory (LSTM) units, ultimately producing a prediction curve indicating earthquake detections at specific time points within the waveform. For training, earthquake detection labels were originally defined from the onset of the manually picked P-wave arrival, extending to a duration of 2.4 times the interval between P- and S-wave arrivals. In cases where datasets lacked S-wave picks or the detections represented teleseismic P-wave arrivals, detection labels were adjusted to begin at the P-wave arrival and extend for 20 seconds after P-wave arrival. The initial training of CRED involved a dataset comprising 550,000 event waveforms and an equal number of waveforms without signal (only seismic noise) collected from Northern California. In this study, CRED was evaluated solely for the earthquake detection task, utilizing the output of the pick detection function.

DeepPhasePick (DPP) is a suite of models designed for earthquake detection and seismic phase picking¹⁸. Its detection module employs a convolutional neural network (CNN) structure utilizing depth-wise separable convolutions, which assign probabilities of noise (N), P-phase (P), or S-phase (S) to 5-second waveform time intervals. The intervals to be classified are extracted close to the earthquake origin times and analyst-picked P- and S-phase arrivals, respectively. The model receives these three-component seismic waveform windows as inputs and outputs three-probability vectors corresponding to the predicted class labels (P, S, or N). Originally, DPP was trained on a dataset comprising 25,647 P-phase waveforms, 14,397 S-phase waveforms, and 25,647 noise waveforms collected around the 1995 Mw = 8.1 Antofagasta and the 2007 Mw = 7.7 Tocopilla earthquakes in Northern Chile. Here, we use the DPP trained on the data from the Italian Seismic Network (INSTANCE)³¹, as models trained on it perform best on average in all tasks³².

Earthquake Transformer (EQTransformer) is a neural network designed for joint earthquake detection, seismic-phase identification, and phase (onsets) picking²⁹. EQTransformer operates on waveform segments of 60 s duration sampled at 100 Hz, outputting three probability prediction traces corresponding respectively to earthquake detection, P-phase, and S-phase

occurrences at each time point within the window. Internally, EQTransformer integrates convolutional neural networks (CNNs), long short-term memory (LSTM) units, and self-attention layers. During training, EQTransformer extensively leverages data augmentation techniques: adding Gaussian noise, inserting random data gaps, and randomly dropping channels. Additionally, EQTransformer performs cyclical time shifts of waveform segments to allow phase picks to appear at arbitrary positions within the window. The labeling of earthquake detection followed the same approach used for CRED. EQTransformer was originally trained on the STEAD dataset²⁸.

Generalized Phase Detection (GPD) is a seismic-phase identification model that analyzes short waveform windows of 4 s duration, sampled at 100 Hz, and classifies each window as P-phase, S-phase, or noise for a single station¹⁴. Although the model is trained using a 2 Hz high-pass filter, it effectively performs across a wide frequency range, demonstrating that the exact training filter is not strictly required when applying the method to new data. GPD primarily performs phase classification, but applying the trained model in a sliding-window approach enables its use for phase onset detection. In the original setup, seismic arrivals were restricted to occur between seconds 1 and 3 of each input window. For inference, the trained GPD model was applied using a sliding-window approach with no overlap. GPD was originally trained and validated using 4.5 million waveform samples from Southern California, evenly distributed among P-phase arrivals, S-phase arrivals, and noise segments. According to Ross et al. (2018), the probability threshold to distinguish events is set to solve specific problems, for example, to create an earthquake catalog minimizing false positives or not to have any false negatives in earthquake early warning¹⁴.

PhaseNet is a U-Net-based deep neural network specifically designed for seismic phase arrival-time picking¹⁷. It processes waveform segments of 30 seconds sampled at 100 Hz, generating continuous probability traces for P- and S-wave arrivals, each of the same duration as the input window. The threshold of probability is set to 0.5 for both P and S picks. Structurally, PhaseNet employs large convolutional filter sizes, incorporates convolutional layers without stride, and utilizes residual connections. The original PhaseNet model was trained and validated on a dataset comprising 779,514 seismic waveforms with labeled P- and S-wave arrivals from Northern California.

FNO-based Model Training

We present a neural operator-based algorithm for the seismic events classification. Fourier Neural Operator (FNO) layers are used to process temporal information using fast Fourier transforms, allowing solutions to be computed quickly. FNO layers are particularly well suited for applications where the domain is a regular grid, which corresponds to the typical structure of seismogram data. Since seismograms are typically sampled at regular time intervals, FNO layers offer an efficient means of processing and encoding this data. A key advantage of neural operators over traditional neural networks is their sample invariance, which allows the input features to be discretized on different grids during each estimation. This eliminates the need for model retraining and allows the algorithm to function efficiently in a variety of seismic recording settings. This property is critical for event detection in dynamic seismic networks, especially for microseismic monitoring, where the acquisition setup may be different for each case study.

We modify the model architecture proposed by Kashafi and Mukerji (2024) for the event classification³³. The FNO architecture used in this study consists of three 1-D spectral convolution blocks (Figure 1). The FNO blocks capture both global and local waveform characteristics, allowing for efficient detection of seismic events in complex time series data exhibiting varying signal-to-noise ratios. Our algorithm takes as input a triggered seismic wavefield recorded with three components at a seismic station and outputs a binary result: 1 - signal, 0 - noise.

The spectral convolution blocks work in the Fourier domain with two important parameters: *modes* and *width*. The *modes* parameter determines how many Fourier modes are retained in each block, with higher-order modes capturing finer details in the data and lower-order modes focusing more on general patterns. The *width* of each block determines the number of features or channels that the network can capture at each layer, which affects the model's ability to learn complex relationships in seismic data, such as amplitude and SNR variations, waveform dispersion.

For earthquake detection, we configure the network with 32 modes and a width of 64 in the FNO blocks. The training process uses the AdamW optimizer with a learning rate of 1×10^{-4} along with the ReduceLROnPlateau scheduler to reduce the learning rate when the validation loss plateaus. The loss function is the binary cross-entropy (BCE), which the model seeks to minimize during training. The seismic events are randomly divided into training (100 one-minute waveforms: 50 signal and 50 noise), validation (same as training), and test (2000 waveforms: 1000 signal and 1000 noise) sets. The validation set is used to fine-tune the learning rate, while the test set is used to evaluate the model's performance.

We used surface monitoring microseismic dataset for training and validation, and adjusted the neural network architecture to have 10 modes and a width of 20 within the Fourier Neural Operator (FNO) blocks. During model training, the AdamW optimizer was employed with an initial learning rate of 1×10^{-3} , complemented by the same ReduceLROnPlateau scheduler. The dataset was randomly divided into three subsets: a training set of 200 one-minute waveforms (100 seismic signals and 100 noise segments), an identical validation set for tuning hyperparameters, and a larger test set of 1000 waveforms (500 seismic signals and 500 noise segments) to rigorously evaluate the predictive performance of the model.

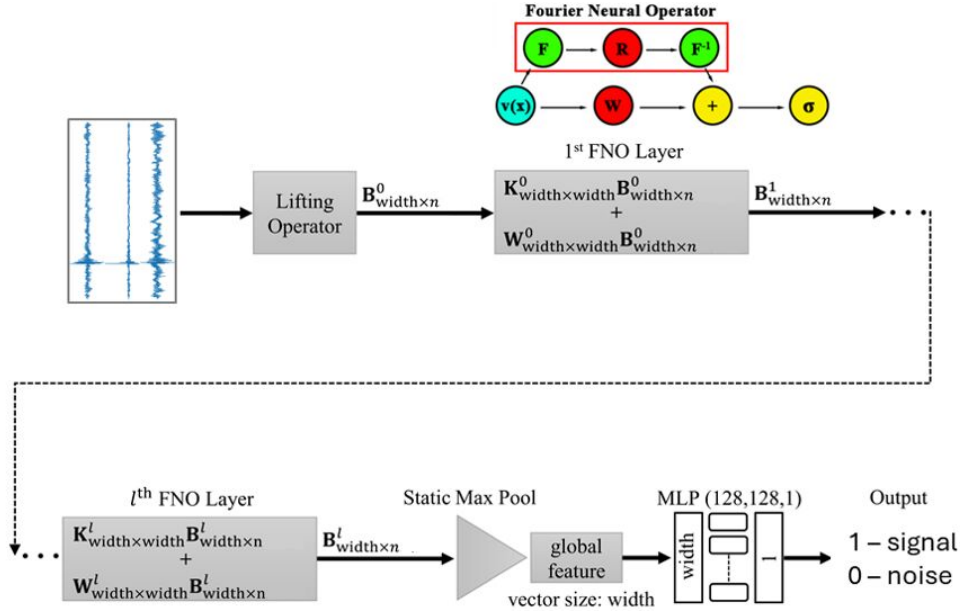


Figure 1. Schematic graph of the proposed FNO-based framework for seismic event detection. The input is a three-component seismic wavefield, and the output is a binary function: 1 - signal, 0 - noise. (adapted after Kashefi and Mukerji (2024)³³)

Evaluation Metrics

Model evaluation is conducted by analyzing the residuals between the ground truth (STEAD or manual labels) and the model's predictions, as well as by computing performance metrics derived from the confusion matrix. Seismic waveforms correctly identified as earthquakes were categorized as true positives (TP), whereas seismic signals incorrectly missed by the model were considered false negatives (FN). Similarly, noise waveforms accurately classified as non-seismic signals were true negatives (TN), and noise signals incorrectly classified as earthquakes were false positives (FP). Based on these results, precision and recall were computed according to Equations 1 and 2, respectively. Furthermore, the F1-score, representing the harmonic mean of precision and recall, was determined following Equation 3. The F1 score depends on a choice of decision threshold. For evaluating seismic event detection performance, we chose the threshold probabilities maximizing the F1 score on the test set independently for each method (Figure 2).

$$\text{precision} = \frac{TP}{TP + FP} \quad (1)$$

$$\text{recall} = \frac{TP}{TP + FN} \quad (2)$$

$$F_1\text{-score} = 2 \times \frac{\text{precision} \times \text{recall}}{\text{precision} + \text{recall}} \quad (3)$$

Results

FNO Model for Earthquake Detection

The training process of the earthquake detection FNO model was conducted over 8 epochs. Here, we show the results for the test set that the trained model did not see before (blind testing). Figure 3 shows the number of true positives, false positives, false negatives, and true negatives obtained by comparing the model output and the labels. The model's performance was measured by metrics such as accuracy, precision, recall, and F1 score. The achieved accuracy on the test set was 95%, precision 94%, recall 96%, and F1 score 95%. These results demonstrate the model's ability to capture data features even with a limited training set of only 100 waveforms. Additionally, the model achieved human-like accuracy in a much shorter time, demonstrating its robustness and efficiency.

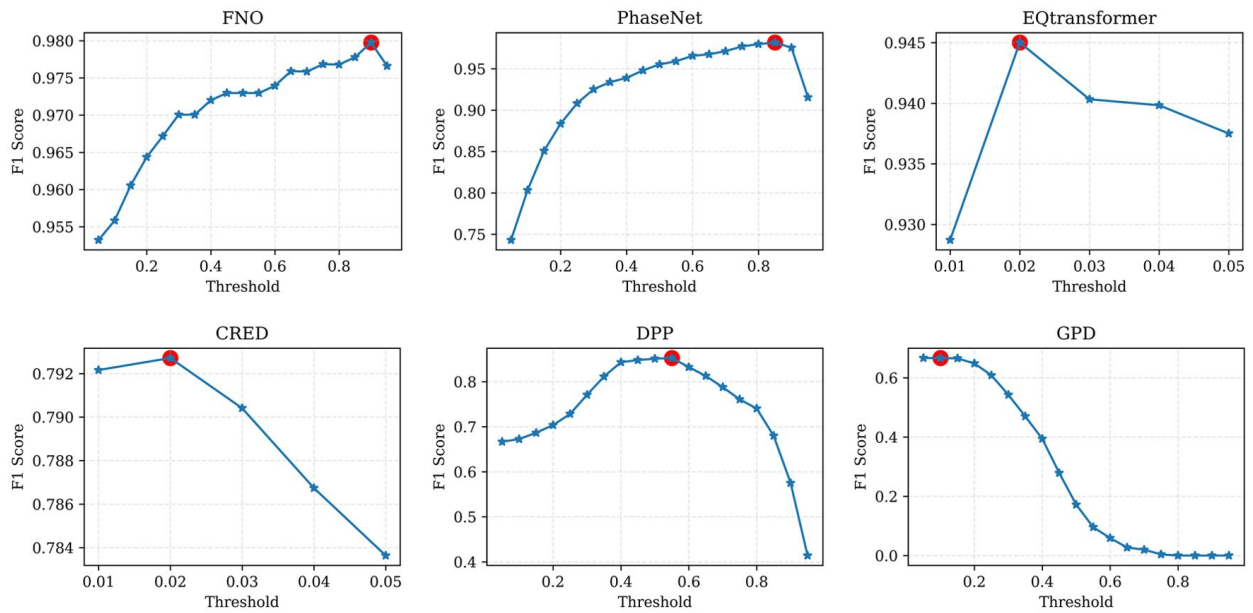


Figure 2. F1 score versus probability threshold results for the test set of 500 random signal and 500 random noise samples from the microseismic dataset. Six deep learning models are evaluated. Trained on a limited number of data, the FNO-based model achieved an F1 score of 0.98.

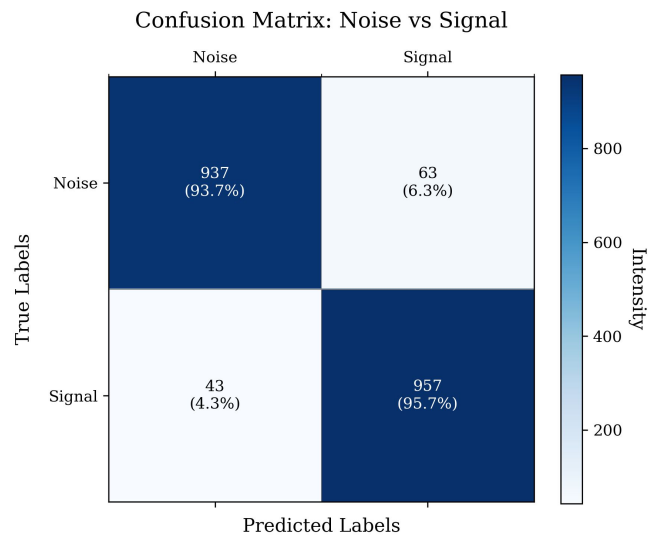


Figure 3. Confusion matrix results for the test set of 1000 random signal and 1000 random noise samples from the STEAD dataset. Trained on a limited number of data, the FNO-based model achieved an F1 score of 0.95.

Microseismic Data Testing

In practical scenarios, models trained on one dataset often need to be applied to different, previously unseen datasets. Performance in such cross-domain applications may differ significantly from performance observed within the original training domain. These differences arise both from variations in seismic data characteristics between the training and target datasets and potential biases introduced by specific annotation methods or data selection processes during training. To assess model robustness in cross-domain conditions, we conducted a cross-evaluation by testing each pre-trained model on the microseismic test dataset (Figure 4). Choosing the optimal threshold, our FNO-based model and PhaseNet achieved the highest performance (F1 = 0.98), closely followed by EQTransformer (F1 = 0.95) (Figure 2). Models with narrower input windows, such as DPP (F1 = 0.85), CRED (F1 = 0.79), and GPD (F1 = 0.67), showed significantly lower scores. This large performance gap highlights the advantage of models such as PhaseNet and EQTransformer, which analyze longer waveforms and thus benefit from a broader temporal context, such as moveout and reflections, to improve phase-identification accuracy.

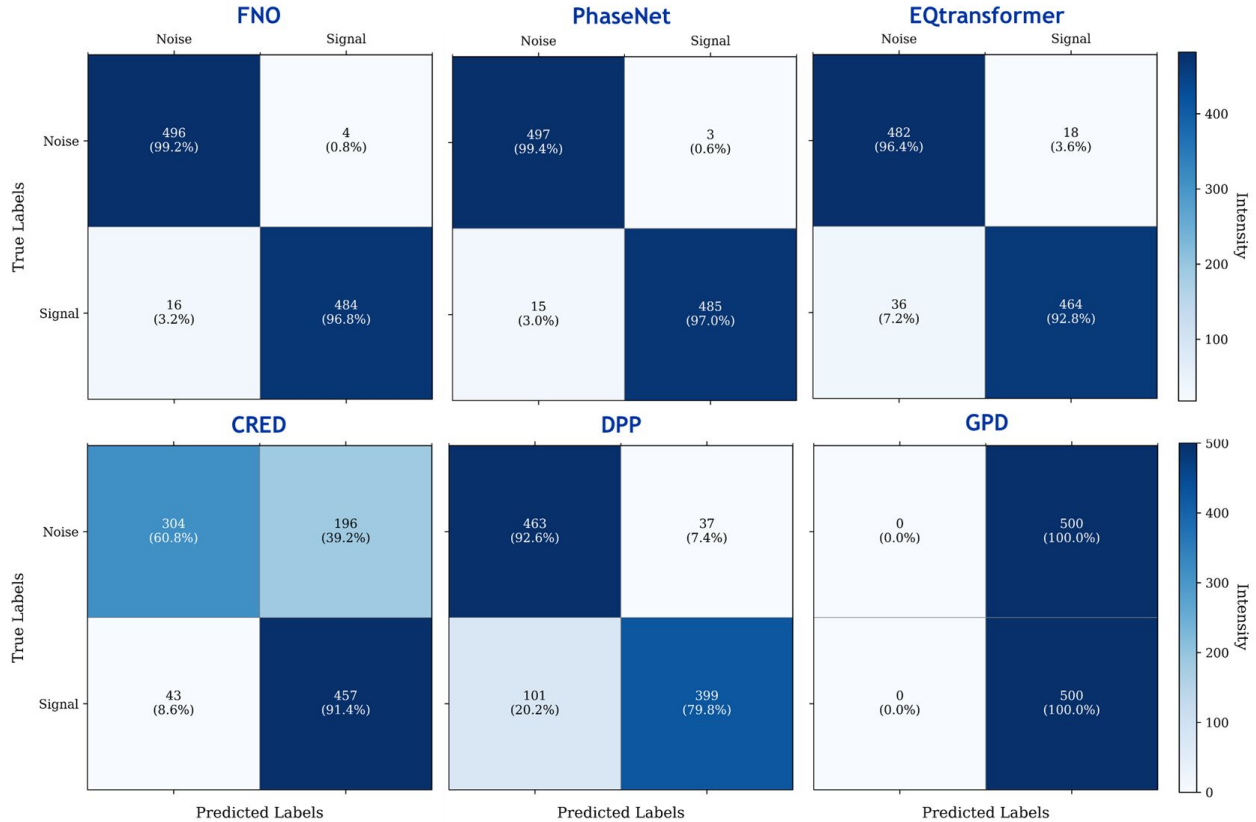


Figure 4. Confusion matrix results for the test set of 500 random signal and 500 random noise samples from the microseismic dataset. Six deep learning models are evaluated. Trained on a limited number of data, the FNO-based model achieved an F1 score of 0.98.

EQTransformer performs better than CRED, which can be explained by the enhanced architecture: EQTransformer is an extended version of CRED that uses attention structures in addition to the CNN and RNN. The poorer performance of DPP may be attributed to its hyperparameters being specifically optimized for a local seismic dataset exhibiting significantly different seismic characteristics. Although the other evaluated models were initially developed using local or regional datasets, their hyperparameters have not undergone the same level of systematic optimization as the DPP model, which may make them more robust when applied to diverse seismic data.

Differences in detection performance between the models may also stem from variations in their definitions of earthquake detections and the nature of the picks within the microseismic dataset. Specifically, GPD, PhaseNet, and DPP determine their detection scores directly from the noise probability, calculated as one minus the predicted noise likelihood. In contrast, CRED and EQTransformer produce explicit detection curves aligned with predefined detection labels that rely on both P- and S-phase annotations. Consequently, especially for regional datasets, these models declare detections only if both P and S annotations are available. In the microseismic dataset, however, certain waveform segments lack either P- or S-wave annotations. This

incomplete labeling may particularly impact the detection accuracy of EQTransformer and CRED.

The deep-learning algorithms evaluated in this study are based primarily on single-station analysis strategies, which may lead to missed detections for events characterized by low signal-to-noise ratios (SNR) or false detections caused by local noise signals with emergent arrivals. To address this limitation and provide a more realistic assessment of practical performance, we additionally compared the models using a seismic array-based voting scheme (Figure 5). Specifically, detections were required to meet a minimum threshold of stations identifying the same seismic event. This approach simulates array-based event detection commonly employed by human analysts, who typically verify seismic events by observing consistent signals across multiple stations.

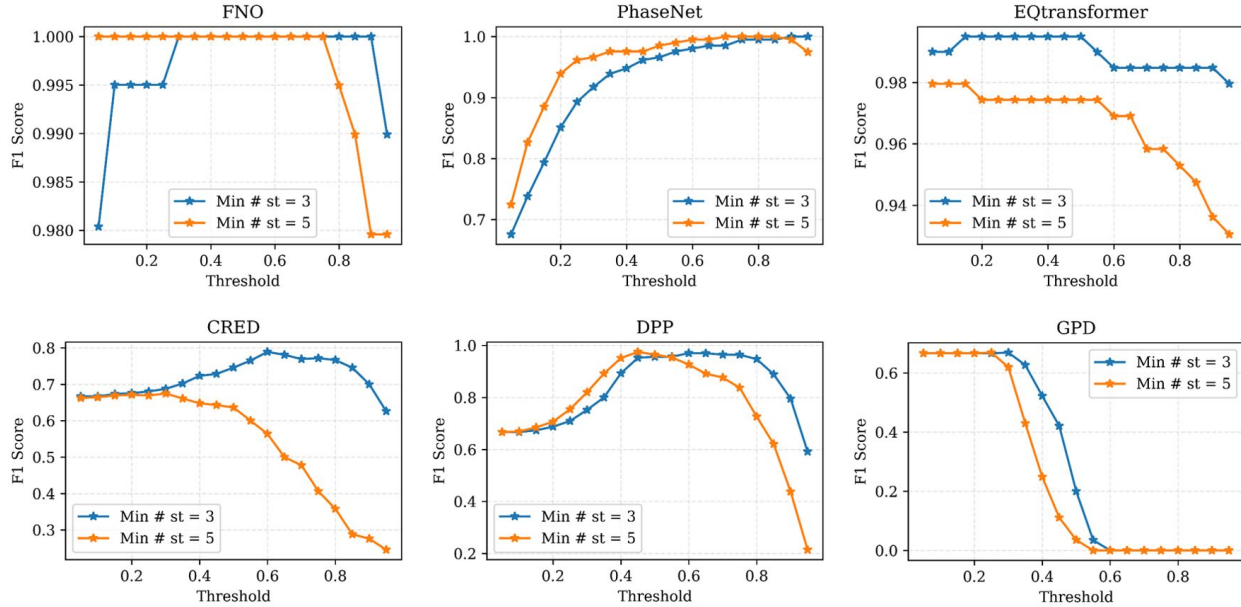


Figure 5. F1 score versus probability threshold results for the test set of 100 random triggered and 100 random false events from the microseismic dataset. Six deep learning models are evaluated. Trained on a limited number of data, the FNO-based model achieved an F1 score of 1.0.

Generally, F1 scores increase with a higher threshold up to a value of threshold value where event detection falls off. The high threshold represents high certainty of detection, but it is not met by low signal events. This is consistent with the fact that the F1 declines faster for a minimum requirement of 5 stations than 3 stations. The increase in the F1 score for low thresholds results from a decrease in the number of false positives. We can conclude that the thresholds for network detection should be chosen based on the number of stations required for detection, as for each method, there is a 'sweet spot'.

We observed significant differences in the F1 scores of different pickers evaluated on the microseismic datasets. This difference most likely stems from the inherent complexity of the detection task for each dataset and the methods used in dataset creation. For example, datasets with lower average signal-to-noise ratio (SNR) inherently present greater detection challenges than datasets with higher SNRs, which may degrade overall performance. Furthermore, inconsistencies in the dataset collection process, such as different quality control standards or annotations provided by multiple analysts, may lead to discrepancies that further decrease model performance. These observations highlight the need to evaluate all models on the same datasets in order to make direct and meaningful comparisons.

Given the latter result, we compared the F1 scores of the different pickers with respect to SNR on our microseismic dataset (Figure 6). We used the vertical component of traces for SNR calculation based on the P phase arrivals. As expected, we observe that pickers have an increasing F1 score with increasing SNR. These results suggest that EQtransformer is more sensitive to SNR than PhaseNet. Overall, the biggest gain of deep learning pickers compared to manual picking is their ability to pick successfully in low SNR conditions.

Discussion

An important factor when choosing deep learning models is their computational requirements. As in most applications, inference time matters more than training time; we do not perform this analysis here.

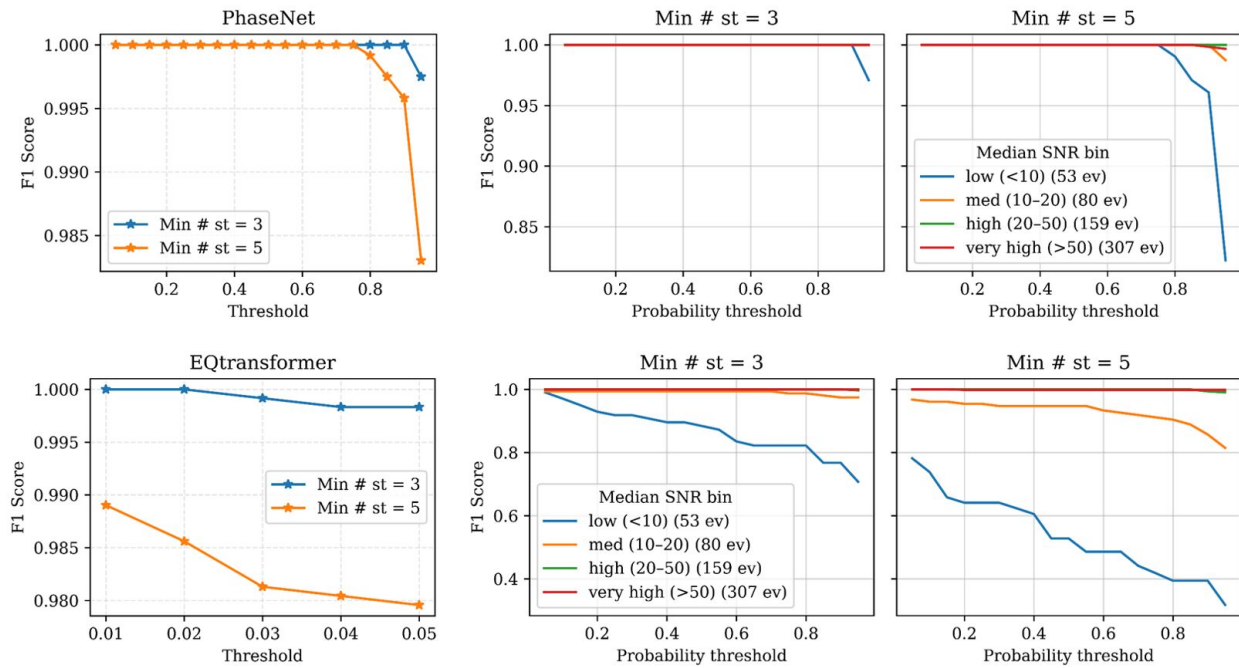


Figure 6. Influence of signal-to-noise ratio on the dependence of F1 score vs. probability threshold. The results are for all microseismic triggered events with 3 and 5 minimum stations voting for signal presence. Two deep learning models are evaluated.

Deep neural networks such as EQTransformer and PhaseNet have significantly advanced earthquake detection and P- and S-phase picking accuracy. However, the complexity of these models limits their practical application in real-time, especially for microseismic monitoring of well operations, which requires lightweight and efficient processing. To address this limitation, we developed an FNO-based detection model, an optimized yet high-performance deep learning model suitable for resource-constrained environments. Training the FNO model typically takes several minutes, depending on the complexity of the operator model and the size of the training set. However, the inference (or testing) time takes less than one second. This makes our approach highly efficient and well-suited for real-time seismic data processing.

Conclusion

We developed and tested a lightweight model based on the Fourier Neural Operator (FNO) for seismic event detection. The model has clear benefits over established automated methods and deep-learning models that need more computational resources. We tested it initially on the STanford EArthquake Dataset (STEAD), and our model performed well ($F1 = 95\%$) even with small training data. Cross-testing with additional microseismic datasets confirmed the robustness and effectiveness of our FNO model. It achieved an F1 score of 98%, reaching and outperforming baseline models such as PhaseNet and EQTransformer, respectively. Our FNO model is lightweight and requires less computational power, a significant advantage when processing real-time data. This makes it very suitable for use in computationally constrained environments such as microseismic monitoring. We show that network detection based on a minimum number of stations that detect a seismic event requires careful choice of the threshold for detection that minimizes the number of false detections while maximizing the number of true detections. FNO methodology appears to be very robust and easy to implement for this purpose.

References

1. Healy, J., Rubey, W., Griggs, D. & Raleigh, C. The denver earthquakes. *Science* **161**, 1301–1310 (1968).
2. Zoback, M. D. *Reservoir geomechanics* (Cambridge university press, 2010).
3. Kivi, I. R., Pujades, E., Rutqvist, J. & Vilarrasa, V. Cooling-induced reactivation of distant faults during long-term geothermal energy production in hot sedimentary aquifers. *Sci. reports* **12**, 2065 (2022).

4. Segall, P. Earthquakes triggered by fluid extraction. *Geology* **17**, 942–946 (1989).
5. Vlek, C. The groningen gasquakes: Foreseeable surprises, complications of hard science, and the search for effective risk communication. *Seismol. Res. Lett.* **90**, 1071–1077 (2019).
6. Kettlety, T., Verdon, J. P., Werner, M. J. & Kendall, J. Stress transfer from opening hydraulic fractures controls the distribution of induced seismicity. *J. Geophys. Res. Solid Earth* **125**, e2019JB018794 (2020).
7. Verdon, J. P. & Bommer, J. J. Green, yellow, red, or out of the blue? an assessment of traffic light schemes to mitigate the impact of hydraulic fracturing-induced seismicity. *J. Seismol.* **25**, 301–326 (2021).
8. Allen, R. V. Automatic earthquake recognition and timing from single traces. *Bull. seismological society Am.* **68**, 1521–1532 (1978).
9. Gibbons, S. J. & Ringdal, F. The detection of low magnitude seismic events using array-based waveform correlation. *Geophys. J. Int.* **165**, 149–166 (2006).
10. Yoon, C. E., O'Reilly, O., Bergen, K. J. & Beroza, G. C. Earthquake detection through computationally efficient similarity search. *Sci. advances* **1**, e1501057 (2015).
11. Gentili, S. & Michelini, A. Automatic picking of p and s phases using a neural tree. *J. Seismol.* **10**, 39–63 (2006).
12. Maity, D., Aminzadeh, F. & Karrenbach, M. Novel hybrid artificial neural network based autopicking workflow for passive seismic data. *Geophys. Prospect.* **62**, 834–847 (2014).
13. Qu, S., Guan, Z., Verschuur, E. & Chen, Y. Automatic high-resolution microseismic event detection via supervised machine learning. *Geophys. J. Int.* **222**, 1881–1895 (2020).
14. Ross, Z. E., Meier, M.-A., Hauksson, E. & Heaton, T. H. Generalized seismic phase detection with deep learning. *Bull. Seismol. Soc. Am.* **108**, 2894–2901 (2018).
15. Mousavi, S. M., Zhu, W., Sheng, Y. & Beroza, G. C. Cred: A deep residual network of convolutional and recurrent units for earthquake signal detection. *Sci. reports* **9**, 10267 (2019).
16. Woollam, J., Rietbrock, A., Bueno, A. & De Angelis, S. Convolutional neural network for seismic phase classification, performance demonstration over a local seismic network. *Seismol. Res. Lett.* **90**, 491–502 (2019).
17. Zhu, W. & Beroza, G. C. Phasenet: a deep-neural-network-based seismic arrival-time picking method. *Geophys. J. Int.* **216**, 261–273 (2019).
18. Soto, H. & Schurr, B. Deepphasepick: A method for detecting and picking seismic phases from local earthquakes based on highly optimized convolutional and recurrent deep neural networks. *Geophys. J. Int.* **227**, 1268–1294 (2021).
19. Wilkins, A. H., Strange, A., Duan, Y. & Luo, X. Identifying microseismic events in a mining scenario using a convolutional neural network. *Comput. & Geosci.* **137**, 104418 (2020).
20. Shaheen, A., Waheed, U. b., Fehler, M., Sokol, L. & Hanafy, S. Groningennet: Deep learning for low-magnitude earthquake detection on a multi-level sensor network. *Sensors* **21**, 8080 (2021).
21. Chen, Y. Automatic microseismic event picking via unsupervised machine learning. *Geophys. J. Int.* **222**, 1750–1764 (2020).
22. Zheng, J., Lu, J., Peng, S. & Jiang, T. An automatic microseismic or acoustic emission arrival identification scheme with deep recurrent neural networks. *Geophys. J. Int.* **212**, 1389–1397 (2018).
23. Birnie, C. & Hansteen, F. Bidirectional recurrent neural networks for seismic event detection. *Geophysics* **87**, KS97–KS111 (2022).
24. Birnie, C., Jarraya, H. & Hansteen, F. An introduction to distributed training of deep neural networks for segmentation tasks with large seismic data sets. *Geophysics* **86**, KS151–KS160 (2021).
25. Awais, M., Hanafy, S. M., Shafiq, S., Al-Shuhail, A. & Waheed, U. B. First break traveltimes picking using unsupervised machine learning and super-virtual refraction interferometry. *Earth Space Sci.* **10**, e2023EA003014 (2023).
26. Kovachki, N. *et al.* Neural operator: Learning maps between function spaces with applications to pdes. *J. Mach. Learn. Res.* **24**, 1–97 (2023).
27. Li, Z. *et al.* Fourier neural operator for parametric partial differential equations. *arXiv preprint arXiv:2010.08895* (2020).
28. Mousavi, S. M., Sheng, Y., Zhu, W. & Beroza, G. C. Stanford earthquake dataset (stead): A global data set of seismic signals for ai. *IEEE Access* (2019).

29. Mousavi, S. M., Ellsworth, W. L., Zhu, W., Chuang, L. Y. & Beroza, G. C. Earthquake transformer—an attentive deep-learning model for simultaneous earthquake detection and phase picking. *Nat. communications* **11**, 3952 (2020).
30. Woollam, J. *et al.* Seisbench—a toolbox for machine learning in seismology. *Seismol. Soc. Am.* **93**, 1695–1709 (2022).
31. Michelini, A. *et al.* Instance—the italian seismic dataset for machine learning. *Earth Syst. Sci. Data* **13**, 5509–5544 (2021).
32. Münchmeyer, J. *et al.* Which picker fits my data? a quantitative evaluation of deep learning based seismic pickers. *J. Geophys. Res. Solid Earth* **127**, e2021JB023499 (2022).
33. Kashefi, A. & Mukerji, T. A novel fourier neural operator framework for classification of multi-sized images: Application to three dimensional digital porous media. *Phys. Fluids* **36** (2024).

Author contributions

Conceptualization: Umair bin Waheed; Data curation: Ayrat Abdullin, Leo Eisner; Formal analysis: Umair bin Waheed, Leo Eisner, Abdullatif Al-Shuhail; Methodology: Ayrat Abdullin, Umair bin Waheed, Leo Eisner; Project administration: Ayrat Abdullin; Resources: Umair bin Waheed, Leo Eisner; Supervision: Umair bin Waheed; Validation: Leo Eisner, Abdullatif Al-Shuhail; Visualization: Ayrat Abdullin; Writing - original draft: Ayrat Abdullin; Writing - review and editing: Ayrat Abdullin, Umair bin Waheed, Leo Eisner, Abdullatif Al-Shuhail.

Data availability

The data supporting the findings of this study are available from Seismik s.r.o., but restrictions apply to their availability. These data were used under license for the current study and are therefore not publicly available. Data are, however, available from the authors upon reasonable request and with permission of Seismik s.r.o.

Competing interests

The authors declare no competing interests.

Funding

The authors received no specific funding for this work.